symmetry

MDPI

Article

Implementation of Finite Element Method Simulation in Control of Additive Manufacturing to Increase Component Strength and Productivity

Miloš Matúš *, Peter Križan, Ján Kijovský, Stanislav Strigáč, Juraj Beniak and Ľubomír Šooš

Faculty of Mechanical Engineering, Slovak University of Technology in Bratislava, Namestie Slobody 17, 81231 Bratislava, Slovakia; peter.krizan@stuba.sk (P.K.); jan.kijovsky@stuba.sk (J.K.); stanislav.strigac@stuba.sk (S.S.); juraj.beniak@stuba.sk (J.B.); lubomir.soos@stuba.sk (Ľ.Š.)
* Correspondence: milos.matus@stuba.sk

Abstract: Additive manufacturing (AM) technologies are becoming a global phenomenon in the manufacturing industry. The progressiveness of additive manufacturing lies in its universality. AM makes it possible to produce parts with complex shapes from different materials without any tools, using only one device. Complex and time-consuming production preparation is eliminated by using AM. It is used in a wide range of industries. Although additive manufacturing is a progressive technology, the currently applied conservative approach has significant limits. The presented work focuses on the development of a new methodology for controlling the AM process. This methodology is based on the outputs of the strength simulation of a specific component through the finite element method (FEM) and their implementation in the printing software of the production equipment. The developed algorithm for controlling the AM process consists of a sequence of successive steps. The designed CAD model of the component is subjected to FEM simulation in order to analyze the von Mises stress in the entire volume of the loaded component. Stresses are distributed asymmetrically in the volume of the component due to the shape and nature of the load. The results of the FEM analysis allow the definition of the volumes in the component with different levels of infill geometry and infill density based on different levels of stress. The FEM simulation also serves to define the effective fiber orientation. The goal of implementing FEM simulation into the building structure of the component is to achieve a symmetrical distribution of stresses in the entire volume. Through the symmetry of internal stresses, it is possible to obtain more efficient production with high productivity and component strength. The work also deals with experimental research on the effect of the building structure on flexural strength. The results of FEM simulation and experimental research are integrated into the developed slicer software to design a layering of the model and the setting of technological and material parameters of printing. This progressive approach makes it possible to generate data for 3D printing based on FEM analysis of components to obtain an optimized printed structure of components and optimized technological and material parameters with regard to maximizing the strength of components and minimizing production times and costs.

Keywords: fused deposition modeling; additive manufacturing; finite element method; 3D printing; fiber orientation; flexural strength

Citation: Matúš, M.; Križan, P.; Kijovský, J.; Strigáč, S.; Beniak, J.; Šooš, Ľ. Implementation of Finite Element Method Simulation in Control of Additive Manufacturing to Increase Component Strength and Productivity. *Symmetry* **2023**, *15*, 2036. https://doi.org/10.3390/sym15112036

Academic Editors: Nikos Mastorakis and Sergei D. Odintsov

Received: 2 October 2023
Revised: 5 November 2023
Accepted: 7 November 2023
Published: 9 November 2023

1. Introduction

Additive manufacturing, as it is known today, has been around for more than 40 years. Its origins can be dated back to the mid-1980s, when the first additive machine, working based on stereolithography, came to the market [1]. According to the standard [2], additive manufacturing is defined as the process of gradually applying and joining material, usually in thin layers, to create a material object from 3D model data [3]. This principle of adding material is the opposite of traditional technologies, in which material is usually removed during the production process [4]. Its use covers a wide range of industries. Its main

application is in the automotive industry [5], aviation, general engineering, space industry, biomedicine [6–9], architecture, fluid technology, etc. This increase in AM applications, together with the decrease in the cost of their implementation, has ensured a tremendous increase in the market for these technologies, and their expansion is expected in the future [4,10].

The key to how AM works is that parts are made by adding material in layers. The original CAD model is divided into the exact number of layers. Each layer represents a thin section of a part derived from the original CAD data. All AM machines use a layer-based approach and differ mainly in the materials that can be used, how the layers are created, and how the layers are bonded together. Such differences will be determined by factors such as the accuracy of the final part plus its material properties and mechanical properties. They will further determine factors such as how quickly the part can be manufactured, how much post-processing is required, the size of the AM machine used, and the total cost of the machine and process [11].

1.1. Pros and Cons of Additive Manufacturing

Among the fundamental advantages of the application of additive manufacturing compared to conventional manufacturing is the possibility of manufacturing very complex shaped parts. Another advantage is achieving better quality and strength properties of the parts (in specific cases). A significant advantage is also a significant saving of material compared to machining. The more complex the shape of the manufactured part, the greater the material savings. Also, significant time savings for technological preparation of production work in favor of additive manufacturing [4,11]. A significant advantage of AM is also the possibility of using different materials in one component or the color resolution of individual parts. AM technologies enable the production of kinematic assemblies without assembly, which in many cases makes it possible to manufacture much more complex assemblies or kinematics that could not be produced with conventional technologies.

Additive manufacturing makes it possible to achieve all the above-mentioned advantages of production, namely the ability to produce complex shaped parts, flexibility, efficiency, precision, and surface quality, as well as the elimination of secondary production times and waste. AM also brings about a fundamental change in the thinking of designers when designing components, as it opens up new possibilities and procedures for their production [4,10].

However, even additive manufacturing technologies have their limits and pitfalls. Among the fundamental ones are often longer production times and, in specific cases, lower production efficiency or higher costs. One of the known disadvantages of AM is the production of components with high surface roughness. This aspect is responsible for a significant reduction in fatigue strength; therefore, it is recommended to apply post-production processes to smooth the surface. In some cases, specific requirements for material treatment enter the production process. For some applications, the input material is more expensive than for conventional production [11].

1.2. Fused Deposition Modeling

Fused deposition modeling (FDM) is a production method based on the use of an external filament (wire) of the thermoplastic material (Figure 1). The filament is unwound from the spool and delivered to the nozzle using an extruder. It is melted in a nozzle that is part of the print head. The print head moves in a horizontal plane and deposits the molten material in one layer. Subsequently, the print head moves by the thickness of the layer and continues to deposit material layer by layer until it has produced the entire component [12,13].

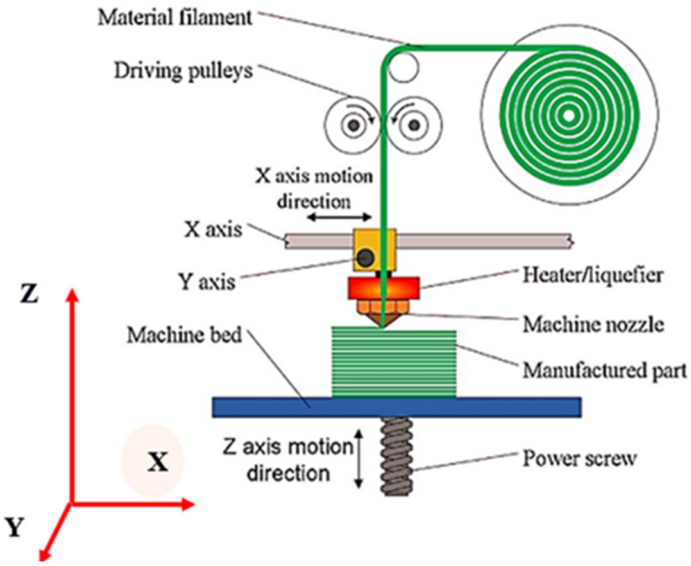

Figure 1. FDM technology [12,13].

The highest print quality is achieved with the smallest layers, but this hits the limits. Each hardware has its limitations in terms of minimum layer thickness. Even if the hardware allows extremely thin layers, the slicer software must divide the CAD model into many layers. A longer time is required to print a thin layer. Furthermore, a larger number of layers is required for a complete CAD model, which multiplies the printing time.

1.3. Structure of the Printed Part

The characteristic structure of objects made by FDM consists of a solid outer shell. This is created by several adjacent grids depending on the wall thickness and the diameter of the nozzle. The density of the outer wall is 100% infill. The internal volume is made up of infill of different geometry and density [14,15]. The infill is used to transfer internal stress and support the external walls. Slicer software–PrusaSlicer 2.6 allows setting the infill density and geometry (Figure 2). This setting is provided manually and depends on the function and load of the printed component. Set infill parameters affect production time and material consumption.

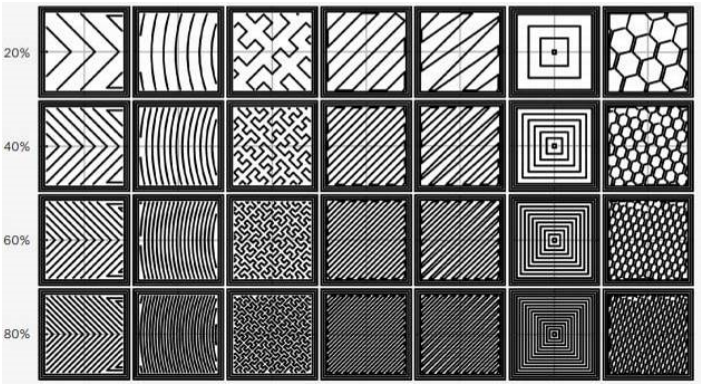

Figure 2. Different infill geometries and their densities [14,15].

Published research on the effect of basic technological parameters on the production process and product properties is very extensive. A lot of scientific papers [16–20] present experimental research on the tensile strength of components produced by additive technologies, especially FDM technology.

In [21], the authors experimentally investigated the tensile strength of ABS samples with respect to fiber direction during FDM printing. The highest tensile strength was obtained when the fibers were laid in the axis of the tensile specimen. The study [22] investigated the mechanical properties of PLA samples through tensile tests and three-point bending tests. Built orientation, printing speed, and layer thickness were variable parameters. The results of the experiments confirmed that samples with fibers in the direction of the axis of the sample achieve higher strength and stiffness. For such a fiber orientation, the strength was also found to increase with decreasing layer thickness and printing speed.

The study [20] experimentally found that the tensile strength decreases with decreasing printing angle. The study [23] investigated the effect of printing parameters such as orientation, infill density, raster angle, and layer thickness on bending strength, tensile strength, and impact strength. The output of this research is in the form of empirical models. In [22], the authors investigated the influence of building orientation on tensile strength and bending strength. The results showed a significant influence of building orientation on the component strength. In [24], the authors performed experiments to define the impact of the building orientation on the mechanical properties of the printing part. To maximize the strength, an optimization algorithm was used to set the printing parameters.

In [25], the authors presented work with experimental research on interlayer shear strength measurement. The obtained results showed that the minimum shear strength of a 3D printing part was one when the shear force was acting along the printing surface.

In studies [19,26,27], the effect of printing orientation on mechanical properties is experimentally investigated. According to an effect of printing orientation, isotropic and anisotropic elastic and yielding models were established.

The effect of the Infill geometry and the percentage of its density on the mechanical properties of 3D printed parts has been discussed in several studies [28–32].

2. Methodology of AM Control Based on Stress Analysis

The mechanical properties of parts manufactured by AM are well investigated. Currently, the challenge in the field of AM is topology optimization. Topology optimization addresses multifaceted problems and plays a pivotal role in tackling the challenges of additive manufacturing. Topology optimization is part of the structural design of parts and is based on a finite element mesh. Its goal is to achieve the required strength of the parts while minimizing the material used for production [33]. Topology optimization is a progressive design tool used to design lightweight, high-performance structures. For functional applications of topological optimization designs, additive manufacturing is primarily used, which can achieve high precision of parts and their structural flexibility [34]. There are many studies devoted to topological optimization for additive manufacturing. These research works focus on shape optimization based on von Mises stress analyses. Alternatively, they also integrate an increase in the local strength of the component by reinforcing with a combination of high-strength materials and fiber vectors. The work [35] explored topology optimization parameter effects on the mechanical responses of an additively manufactured component structure. Studies [36–38] focus on the topology optimization method in order to reinforce critically loaded volumes of the component by using a fiber placement design of carbon-fiber-reinforced plastic (CFRP). The study [37] presents a novel non-parametric shape-topology optimization method for fiber placement and orientation design, aiming at controlling the stiffness of CFRP but in shell structures. The solid isotropic material with the penalization method is employed for topology optimization. The gradient functions derived are applied to the H1 gradient method for fibers to determine the optimal shape and topology. The results obtained in the investigation [38] indicate that it is essential to comprehensively consider the AM process-induced microscale material anisotropy and mesoscale geometric errors in the topology optimization of fiber-reinforced polymer lattice structures to improve the accuracy and reliability of the optimal design. Research with a similar goal aimed at reinforcing critically loaded volumes of the component was also

published in the next work. The study [34] deals with the fabrication of structures in which members made of multiple materials are placed in appropriate positions. This paper proposes a topology optimization method that considers the dimensional constraints of each material component. An extended level-set method is used to represent multiple material phases in the structural design. The state of the art of topology optimization is processed in great detail in the work [39]. The review is focused on topology optimization for additive/subtractive manufacturing; the existing methods are thoroughly reviewed, and their potential to address design for hybrid additive manufacturing issues is carefully analyzed.

The common output of topology optimization is a modified final shape of the component. However, for some applications, it is necessary to keep the original shape of the component. This is the primary motivation for the development of this new methodology. The presented methodology is intended for the usual FDM production of solid components in the engineering industry from various plastic materials. The development of this methodology is the subject of the research activities presented in this work. Based on this methodology, the strength of structured components manufactured by FDM will be predictable with good precision. Later, it will be possible to expand it to other technologies of additive manufacturing. This methodology represents an algorithm for the design of a software tool. It allows setting all parameters that affect the functionality and strength of components already in the process of preparing and generating manufacturing data, such as G-codes for additive manufacturing equipment.

This data is directly correlated with the production time of the components. The different infill geometry and density, the complexity of the structure of the manufactured component, as well as the thickness of the applied layers directly affect the production time. For this reason, it is desired to investigate the optimal condition between the mentioned parameters for industrial applications. Because the final component must achieve the required strength, and its production must take a minimum time [40].

The methodology for controlling the AM process is based on the integration of the outputs of the strength analysis into the printing software of the production equipment. The developed algorithm is based on several subsequent steps. The strength analysis is used for solving the CAD model of the printed part by the finite element method (FEM). It is clear from the FEM results that the stresses are inhomogeneously distributed in the volume of the component. The methodology of the algorithm is based on dividing the part into separate volume areas with different stress levels. These separate volumes can be produced by AM with different printing orientations and different types and densities of infill. The results of a von Mises stress analysis will be integrated into the slicer software to design a layering of the model and the setting of technological and material parameters of printing.

A lightweight, low-density infill will be designed for low-stress areas. This reduces production time and material. On the contrary, the software will propose optimal technological and possibly material parameters (fiber diameter, printing speed, temperature, and type of material) for volume areas with higher levels of stress.

The goal is to generate data in the form of G-codes for the optimized printed structure of the component to maximize its strength and minimize production time and costs.

3. Application of FEM Tools in Control of Additive Manufacturing

3.1. Finite Element Method

The finite element method is a numerical method used to simulate structural analysis, deformation, natural frequencies, heat flow, etc., on the created physical model. Its principle consists of the discretization of a continuous continuum into a finite number of elements while the detected parameters are determined at individual nodal points. FEM is primarily used to check already designed components or to determine the critical location of the structure [41]. This study finds applications in many fields during product development, usually in the field of mechanical engineering (e.g., aerospace and automotive industries and biomechanics).

The finite element method is a basic tool that can be appropriately used and integrated into the design of optimization slicer software for additive manufacturing to make production more efficient. FEM application saves manufacturing time, cost, and mass and can increase strength by highlighting problems and finding solutions early in the component design phase.

The finite element method is based on Lagrange's principle: the body is in equilibrium if the total potential energy of the deformation of the system is minimal. The FEM application procedure is as follows:

1. CAD model.
2. Discretization of the model (replacement of the continuous volume of the model with a finite number of elements or nodal points).
3. For each discrete point, we obtain three equations—displacement field in all directions (x, y, z)—and we try to calculate the deformation field (six equations) and von Mises stress field (six equations).
4. Replacing the displacement function with a polynomial and expressing the displacement function.
5. Introduction of boundary conditions.
6. Calculation of a system of linear algebraic equations.
7. Calculation of deformations and stresses for individual nodal points.
8. Mostly graphic display on the model with a list of important values.

3.2. Loading of a Simple Beam Made by FDM

A loaded simple beam will be used for a detailed explanation of the hypothesis and procedure. A simple beam can be fixed and loaded in different ways. A simply supported beam is a beam that is supported at both ends. The external loading force pushes the beam to the center of its length. Figure 3 shows how the beam is curving by acting the force.

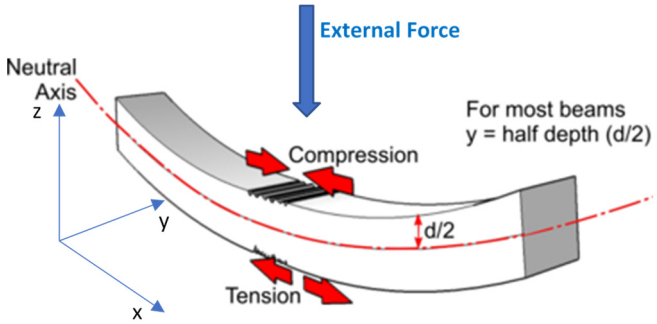

Figure 3. Simply supported beam load.

The volume above the neutral axis is compressed. If this part is created by laying fibers in the x–y plane using FDM technology, then the vector of these fibers must be perpendicular to the neutral axis to achieve maximum strength. If the fibers are printed in the direction of the neutral axis, each fiber would be under buckling stress, which could cause damage. The volume below the neutral axis is under tensile stress, then the vector of these fibers must be parallel to the neutral axis to achieve maximum tensile strength. If the fibers are printed in the opposite direction-perpendicular to the neutral axis, they will be pulled apart [40].

The cantilever beam has one end fixed, and the second end is free, as shown in Figure 4. The external force acts on the free end of the beam in the z-axis direction. The cantilever beam has curvature in the opposite direction to a simply supported beam when subjected to a force with the same vector. Thus, the area of compression and tension is oriented opposite to the neutral axis. It is also necessary to adjust the fiber deposition direction during the production of the component using FDM technology. If the fibers forming the volume above the neutral axis are placed in the x-axis direction (parallel to the neutral axis), this volume will reach maximum tensile strength. The volume below the neutral axis is

compressed, then the vector of these fibers must be perpendicular to the neutral axis (in the *y*-axis direction) to achieve maximum compressive strength [40].

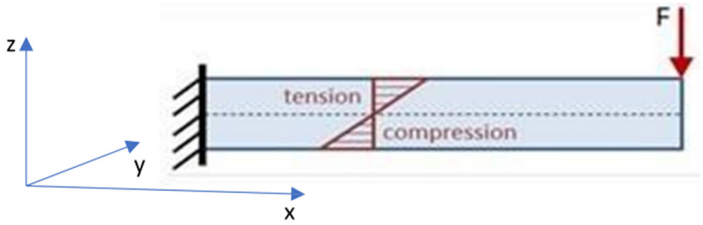

Figure 4. Cantilever beam load.

3.3. Strength Analysis Based on FEM Simulation

The FEM analysis will be used as a tool for identifying different von Mises stress levels as well as stress directional vectors (compressive and tensile) in the loaded component. The stress distribution in the volume of the component is usually asymmetric. Then, it is possible to divide the investigated component into separate volumes with the corresponding stress level and vector. This procedure can be applied in the control of the additive manufacturing process—for FDM technology. Optimal technological parameters, infill geometry, and infill density will be assigned for each volume area so that there is a symmetrical stress distribution in the real component. This means that a higher homogeneity of the stress distribution will be achieved in terms of the magnitude of the stress values. Likewise, a better level of symmetry of tensile and compressive stresses distributed in the volume of the component will be achieved. The exact procedure is applied and described in detail on the real component—draw bar in Figure 5, where green arrows mean fixed geometry, purple arrows mean external load. This type of real-used component was chosen as an example for a clear explanation of developing methodology for slicer software.

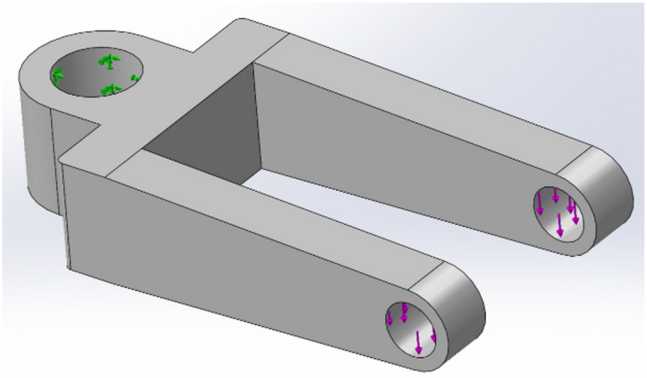

Figure 5. Loaded CAD model of the drawbar (green arrows mean fixed geometry, purple arrows mean external load).

Stress is created in the component by the action of an external load. CAD software SolidWorks 2022 was used for modeling and strength analysis. The following settings were used for the analyzed component: an ABS material with filament manufacturer specification, a standard mesh with an element size of 1.5 mm (Figure 6), a total number of mesh elements of 507,344, a loading force of 60 N, and fixture details—fixed geometry. The obtained and further processed output was von Mises normal stress. For further assessment, only qualitative analysis is used to define stress vectors and stress levels. Calculation software working based on FEM displays the stress in the entire volume of the CAD model with a color scale (Figure 7). Cold colors represent the component volume with low stress. Warm colors represent the component volume with high stress. The red volume represents the maximum von Mises stress.

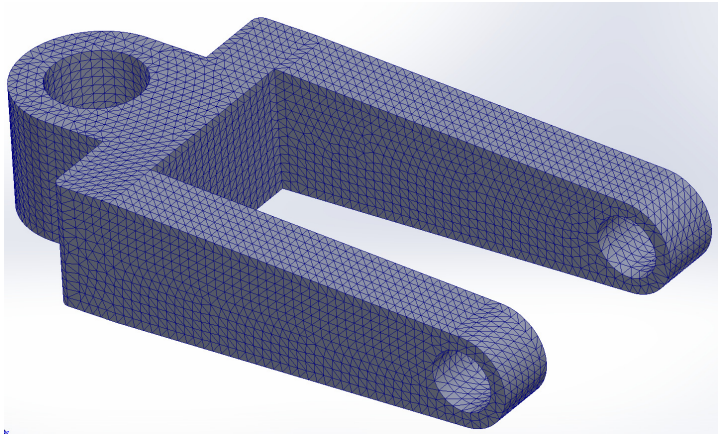

Figure 6. The mesh of the CAD model.

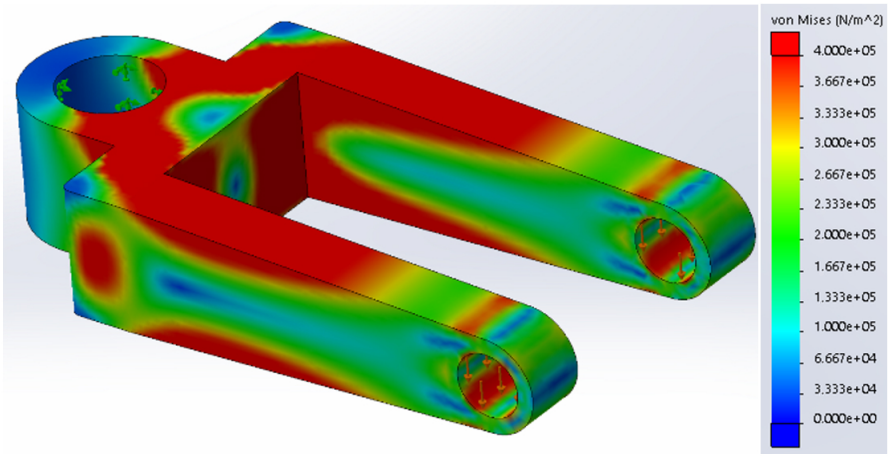

Figure 7. Von Mises stress simulation of the drawbar model.

There is a very simple symmetrical stress distribution in the simple beam. The stress decreases from the surface to the middle of its thickness. It is possible to observe a blue area along the beam in the middle of a thickness (Figure 8). The blue horizontal plane is called the "zero plane". It represents a thin volume where there is zero stress. The zero plane divides the beam volume into two halves with opposite stress vectors. The fibers in the volume area above the zero plane are pulled, so there is a tensile stress. On the other side, fibers in the volume area below the zero plane are compressed, so there is compressive stress.

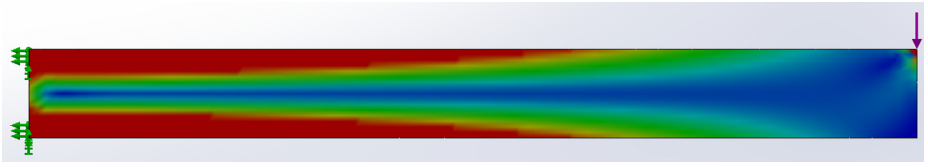

Figure 8. Von Mises symmetrical stress distribution of the simple beam—perpendicular projection.

When applying FEM to a real part (Figures 7 and 9), an analogy can be seen, but the course of stress in the volume of the rod is already more complex and asymmetric. When creating the structure of a simple beam, it is possible to predict the course of stress based on the theory of elasticity and strength. For more complex components, it is necessary to use MKP software SolidWorks 2022 applications.

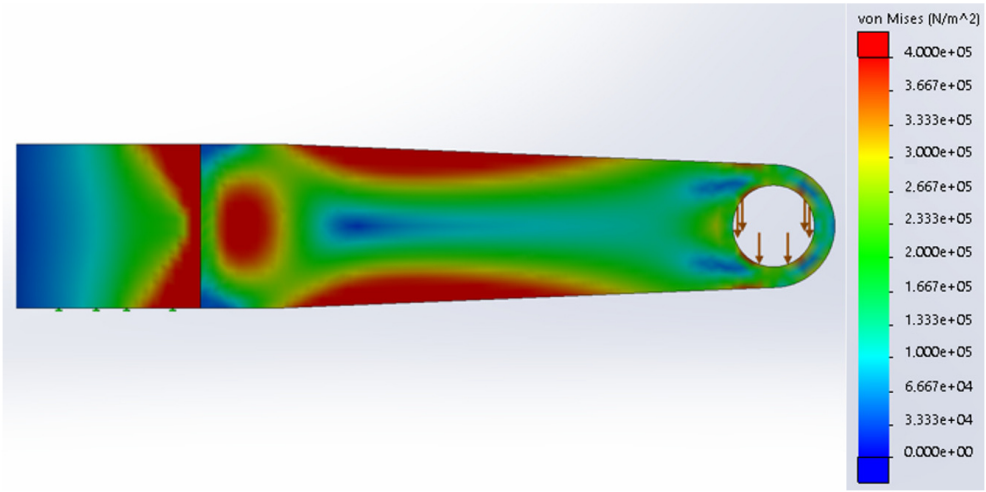

Figure 9. Stress simulation of the drawbar—perpendicular projection.

3.4. Infill Geometry and Infill Density Based on Different Levels of Von Mises Stress

A fundamental point of the developed methodology is the determination of individual von Mises stress levels across the volume of the loaded part. FEM makes this possible. The component is divided into individual separate volumes, each with a different stress level. And so, in practice, the software determines the optimal printing parameters for each volume separately to achieve the required strength and minimize production time and material. The infill of suitable geometry and low density will be implemented for volumes of low-stress levels to save production time and the amount of construction material. Volumes of the component with high-stress values will be produced with the optimal setting of technological and material parameters by applying FEM simulation, and thus the efficient production of a high-strength component will be achieved [40].

The FEM simulation uses different tools for defining and investigating different stress areas in the component. Very useful are tools for the investigation of stress levels inside the mass of the component, such as various sections, stress levels, Iso clipping, etc. The presented methodology applies these FEM tools in the development of optimization slicer software. The basic principle is the separation of individual volumes of the 3D model of the manufactured component based on predefined stress levels using FEM simulation. For each defined stress level, the particular volume of the model is separated, and the optimal parameters of effective production are defined from the point of view of strength, production time, and material consumption. Tools such as the Iso Clipping and Iso Section are intended for researching any set stress level in the volume of the CAD model. This tool allows to efficiently define and separate the volume of a component subject to a defined range of stress. Examples of the implementation of these FEM tools are given for a specific component—the drawbar.

Figure 10 shows the drawbar volume where the level of stress is higher than 90% of the maximum stress. To achieve maximum strength, this separated volume should be printed as solid with 100% infill. The output of the analysis for each defined range of stress level is also information about the percentage of the separated volume to the total volume of the component. This investigated volume with 100% infill represents 32% of the total volume. It is not only important to optimize the structure of the component but also to optimize the setting of the technological and material parameters of the print.

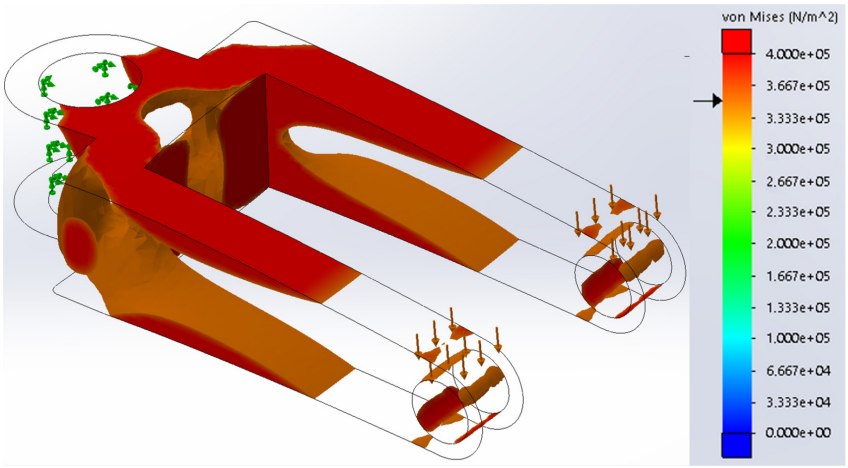

Figure 10. Component volume with the von Mises stress level over 90% of the maximum stress.

The parts of the component that have stress levels between 50% and 90% of the maximum stress value are shown in Figure 11. According to this presented method, the slicer software chooses to make the inside of the component more filled up or completely solid, depending on the printing settings that will make it strong and fast. The best printing settings are determined by the material's properties, the external force applied, and the findings from experiments.

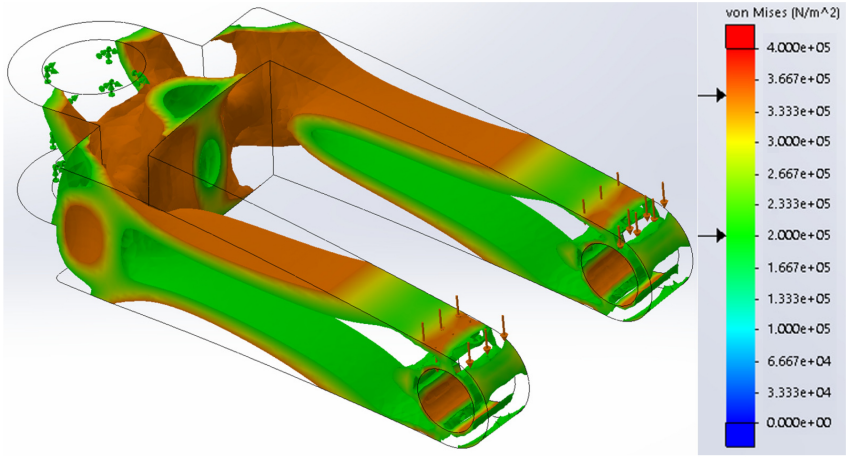

Figure 11. Component volume with the von Mises stress level between 50% and 90% of maximum stress.

Based on this methodology, the slicer software can decide to create the volume area, where the von Mises stress reaches up to, e.g., 30% (Figure 12), as an infill with a very low density. In component volumes with very low stress, it is possible to significantly reduce the infill without affecting the structural integrity of the part. The application of this method significantly reduces material usage, costs, and production time.

Although additive manufacturing is a progressive technology, the currently applied conservative approach has significant limits. However, these limits can be removed in software by implementing the mentioned methodology. The goal of implementing FEM simulation into the building structure of the component is to achieve a symmetrical distribution of stresses in the entire volume. Through the symmetry of internal stresses, it is possible to obtain more efficient production with high productivity and component strength. The implementation of FEM results into printing software significantly reduces production times, costs, the amount of material used, as well as mass while maintaining the required strength and shape.

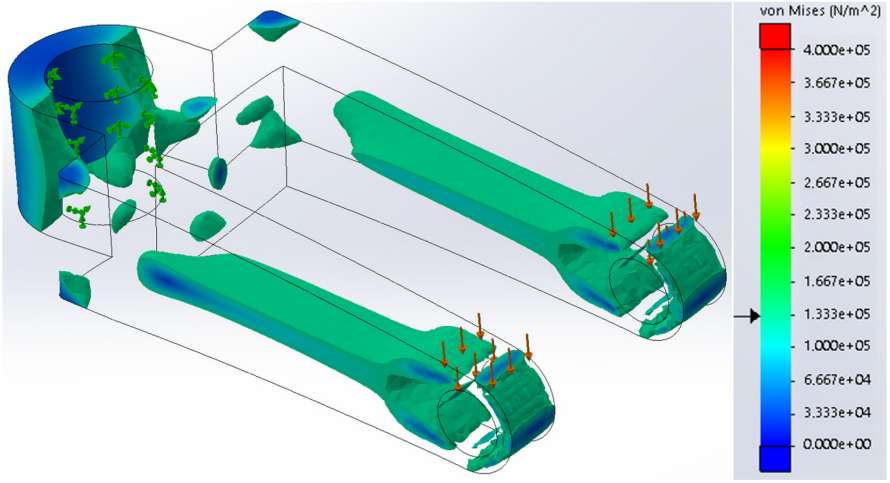

Figure 12. Lightened volume with von Mises stress lower than 30% of maximum stress.

3.5. Orientation of Fibers Based on FEM Simulation

The orientation of the printed fibers in the component significantly affects its strength. As already mentioned above, the results of experiments by many authors have shown that the orientation of the fibers needs to be paid due attention. The highest tensile strength is achieved with fibers oriented parallel to the neutral axis. The highest compressive strength is achieved with fibers oriented in a direction perpendicular to the neutral axis.

While performing FEM analysis, it is necessary to find where the compressive stress and tensile stress are in the part volume. This is necessary to decide the layout of the fiber during the 3D printing of part by FDM.

In Figures 13 and 14, it can be observed that the green color is the low-stress level around zero. The warm color is tensile stress (+), and the cold color is compressive stress (−). So, in such a way, it is possible to identify part volumes with tensile and compressive stress. It is a very useful function to decide the direction of fibers during FDM. Figure 15 shows the results of the FEM analysis focused on the stress vector as the complete volume with tensile stress. Figure 16 represents the volume with compressive stress in the component.

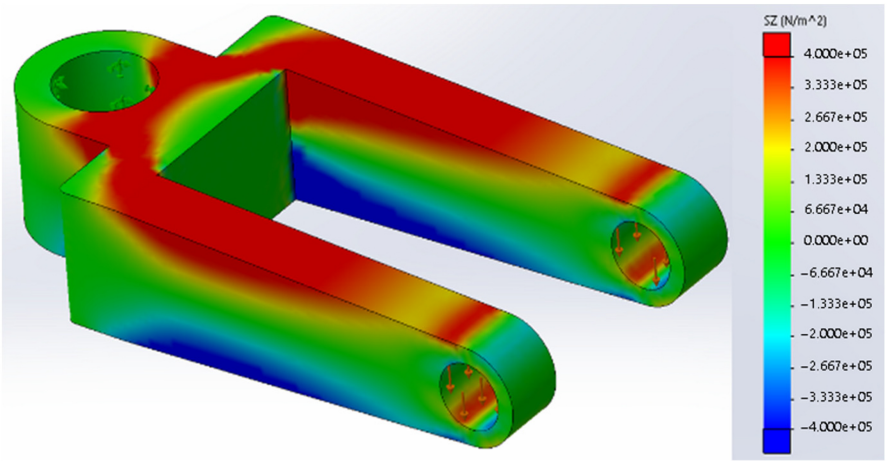

Figure 13. Investigation of compressive and tensile stress.

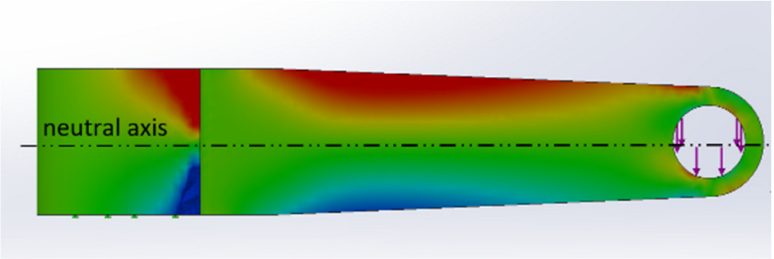

Figure 14. Neutral axis dividing stress vectors symmetrically—perpendicular projection.

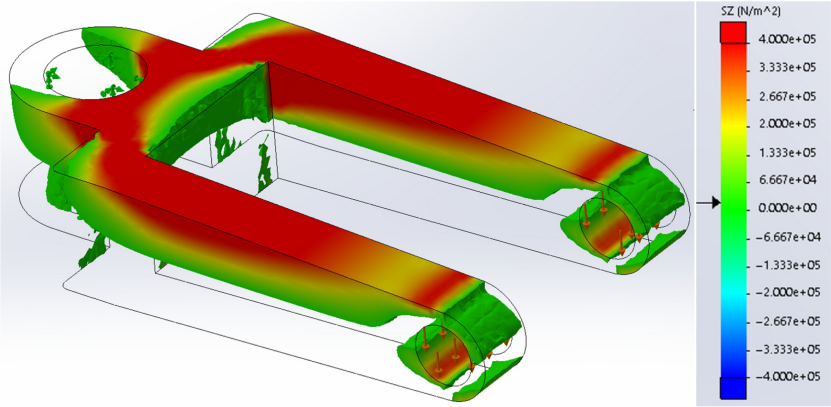

Figure 15. Component volume with tensile stress.

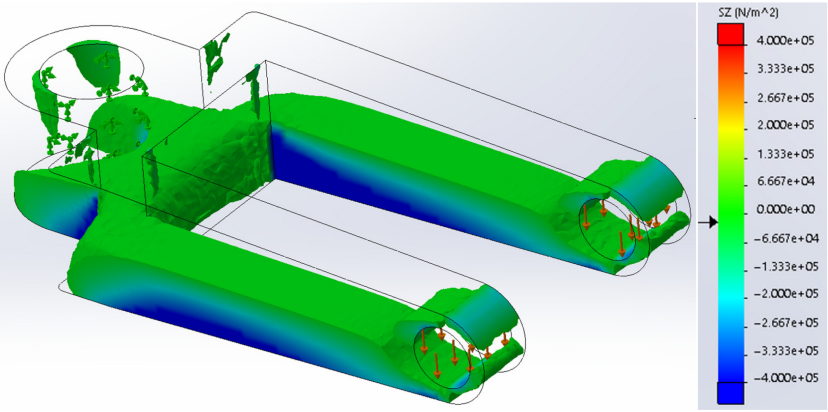

Figure 16. Component volume with compressive stress.

The strength of the component can be significantly increased by the correct orientation of the printed fibers by implementing these FEM results. With the correct orientation of the fibers, it is even possible to increase the overall strength even with light infill compared to conventionally printed components with 100% infill with fibers in the same orientation.

4. Flexural Strength Experimental Verification

The confirmation and support of the mentioned methodology for AM controlling is based on the experimental tests performed to define the bending strength for different structures of the components produced by AM. The experiments confirm the scientific hypothesis of the influence of fiber orientation, density, and structure of the filling.

4.1. Material and Methods

Apart from the technological parameters of the AM process, it is the material that significantly affects the mechanical properties of the components produced by FDM. For the experimental verification of the effect of the components' structure (orientation of fibers,

infill geometry, and infill density) on their bending strength, a common thermoplastic material, polyethylene terephthalate glycol (PETG), was used.

The experimental tests were designed and provided according to the standard [42]. Testing flexural specimens were designed in the shape of a block with dimensions of 10 × 8 × 80 mm ($b \times h \times l$). An amount of 4 different samples in 6 pieces (a total of 24 samples) were printed with structures according to Table 1.

Table 1. Structures of tested samples.

Sample	Structure by Height (8 mm)
A	100% Transverse fibers (16 layers)
B	100% Longitudinal fibers (16 layers)
C	50% Transverse fibers (8 top layers) and 50% longitudinal fibers (8 bottom layers)
D	25% Transverse fibers (4 top layers) and 50% honeycomb infill (8 middle layers) and 25% longitudinal fibers (4 bottom layers)

The samples were fabricated by an Original Prusa i3 MK3S+ FDM 3D printer. Set process parameters via the software PrusaSlicer 2.6 for four different types of samples are defined in Tables 2 and 3. To demonstrate the proposed methodology for increasing productivity, rough printing settings were used, i.e., large nozzle diameter, high layer, high printing speed, etc. A side view of the structure of real printed samples is shown in Figure 17. There, it is possible to observe the distribution of layers according to the height of the specimens. Roughing printing naturally reduces the adhesion and diffusion of particular layers and thus has a negative effect on the strength characteristics of printed parts. On the other hand, the productivity of production is increasing rapidly. Therefore, the main goal of the research is to investigate the influence of the building structure on the strength characteristics of printed parts.

Table 2. Process parameters of samples with simple structure.

Parameters	Sample A	Sample B
Nozzle diameter	0.80 mm	0.80 mm
Building orientation	Flat	Flat
Layer thickness	0.55 mm	0.55 mm
Top solid layers	0 layers	0 layers
Bottom solid layers	0 layers	0 layers
Outline perimeters shell	0 outlines	0 outlines
Internal fill pattern	Aligned Rectilinear	Aligned Rectilinear
Top fill pattern	Aligned Rectilinear	Aligned Rectilinear
Bottom fill pattern	Aligned Rectilinear	Aligned Rectilinear
Internal fill percentage	100%	100%
Fill angle	0°	90°
Extruder temperature	250 °C	250 °C
Heated bed temperature	90 °C	90 °C
Default printing speed	50 mm·s^{-1}	50 mm·s^{-1}
Filament diameter	1.75 mm	1.75 mm
Filament density	1.27 g·cm^{-3}	1.27 g·cm^{-3}
Total printing time	45 min	36 min

Table 3. Process parameters of samples with combined structure.

Parameters	Sample C	Sample D
Nozzle diameter	0.80 mm	0.80 mm
Building orientation	Flat	Flat
Layer thickness	0.55 mm	0.55 mm
Top solid layers	0 layers	0 layers
Bottom solid layers	0 layers	0 layers
Outline perimeters shell	0 outlines	0 outlines
Internal fill pattern	Aligned Rectilinear	Aligned Rectilinear
Internal fill pattern of central part	-	Honeycomb
Top fill pattern	Aligned Rectilinear	Aligned Rectilinear
Bottom fill pattern	Aligned Rectilinear	Aligned Rectilinear
Internal fill percentage	100%	100%
Internal fill percentage of central part	-	40%
Fill angle of longitudinal part	90°	90°
Fill angle of transverse part	0°	0°
Fill angle of central part	-	45°
Extruder temperature	250 °C	250 °C
Heated bed temperature	90 °C	90 °C
Default printing speed	50 mm/s	50 mm/s
Filament diameter	1.75 mm	1.75 mm
Filament density	1.27 g/cm^3	1.27 g/cm^3
Total printing time	41 min	45 min

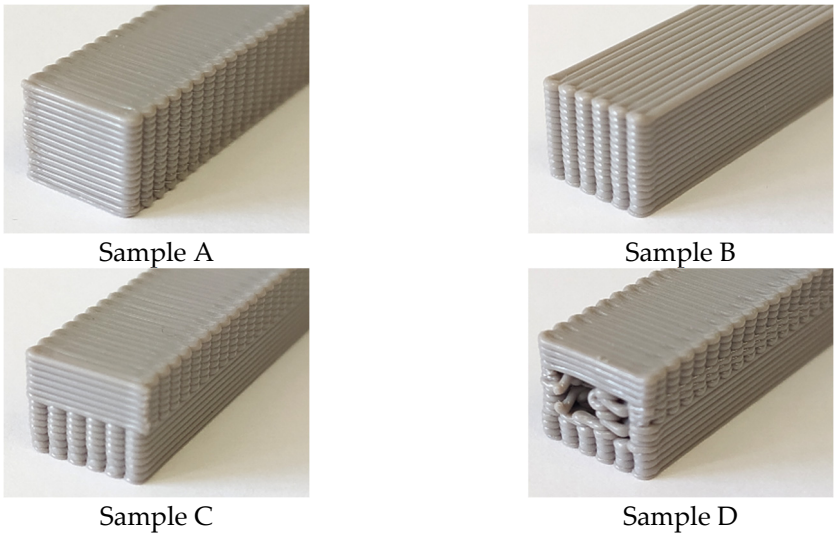

Figure 17. Structure of printed samples.

Specimens were tested on the universal testing machine Inspekt 5 Desk. The method used to determine the maximum bending stress (flexural strength) of samples is based on a three-point bending test. The specimen was placed on two supports 64 mm apart. The load through the punch was applied to the specimen in the middle between the supports

(Figure 18). The radius of the supports and the punch was 5 mm. The loading speed was set to 1 mm/min. Tests were performed in stable laboratory conditions (20 °C and 50% humidity). Also, the samples were acclimatized for 48 h in these conditions.

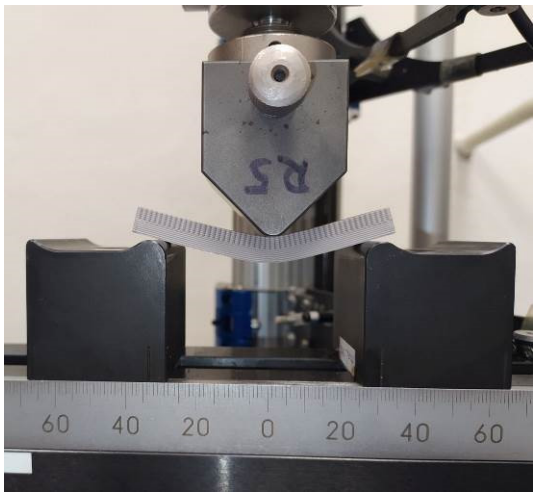

Figure 18. Flectural strength test on universal testing machine Inspekt 5 Desk.

The flexural strength of each sample was calculated according to the standard [42]:

$$\sigma_f = \frac{3FL}{2bh^2} \quad (1)$$

This function represents the relationship between the examined flexural strength σ_f, the maximum loading force F (N), the distance between the supports L (mm), the width of the specimen b (mm), and the height of the specimen h (mm).

It was also necessary to measure the exact mass of individual samples with different structures to correctly draw the conclusions of the experiments.

4.2. Results and Discussion

The flexural strength test was realized for 24 specimens (6 specimens for each sample). The measured flexural strength values, as well as exact mass, were statistically evaluated. For each sample, the arithmetic average of the measured values was calculated, and the standard deviation was determined. The results for each sample are shown in Table 4.

Table 4. Results of flexural strength, mass, and ratios for all samples.

Sample	A	B	C	D
Flexural strength (MPa)	47.03	61.86	62.02	53.68
Mass (g)	7.2632	7.4485	7.3068	6.0678
Strength/Mass ratio (MPa·g^{-1})	6.48	8.31	8.49	8.85
Strength ratio D/C (%)	-	-	-	86.55
Mass ratio D/C (%)	-	-	-	83.04

It is clear from the results of the experimental research that the maximum flexural strength value was achieved by the building structure of Sample C; however, Figure 19 shows that Sample B had a very similar result. As expected, Sample A achieved the lowest value of flexural strength. Sample D achieved a lower, but not the lowest, value of flexural strength compared to Sample C, which was due to the lightened core structure.

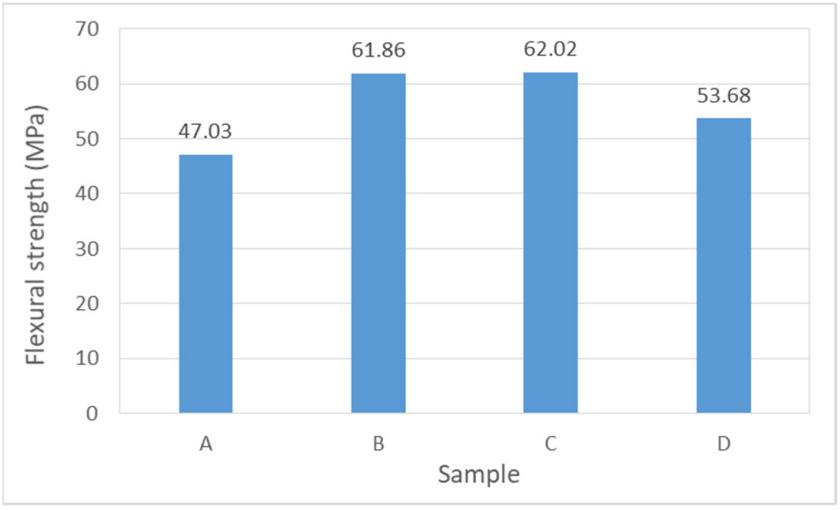

Figure 19. Maximum flexural strength of the samples.

The same 3D model with the same dimensions was used to print all the samples. However, the building structure (given by the different fiber orientations, types, and infill densities) can significantly affect the mass of individual samples. As Figure 20 shows, the maximum mass of samples was reached by Sample B, but Samples A, B, and C had very similar masses. However, Sample D, which has a lighter structure (only 40% infill density), reached a significantly lower mass. Low mass is required for high productivity of production. Lower mass means lower production times and lower costs for production and material.

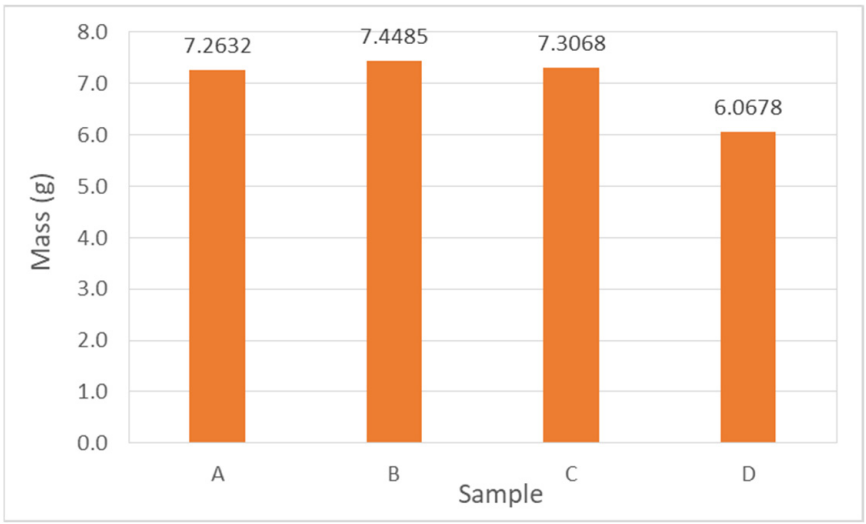

Figure 20. Average masses of the samples with different structures.

For the correct evaluation of an effective building structure, it is necessary to take into account the maximum flexural strength in comparison with the mass of the structure. Table 4 also shows the calculated strength/mass ratio. This ratio represents the value of the load that one gram of the structure is able to carry. Figure 21 compares values of this ratio for individual samples with different building structures. From the results of the strength/mass ratio based on experimental research, it can be concluded that Sample D has the most efficient building structure of the samples considered. This means that the structure of Sample D will carry the largest bending load per unit mass.

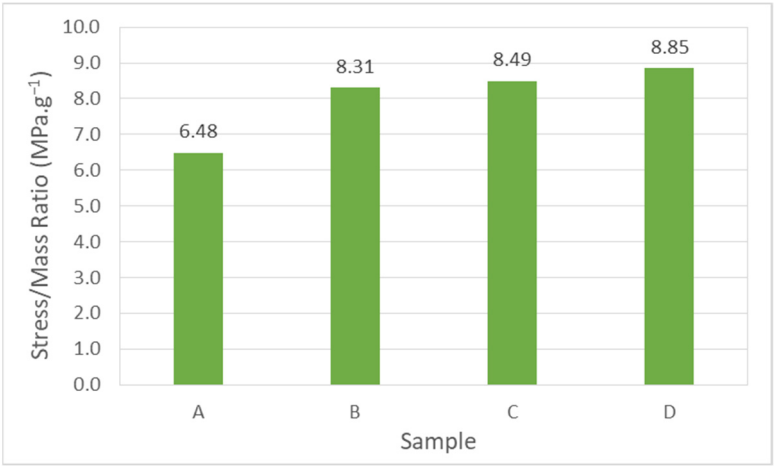

Figure 21. Strength/mass ratios of the samples.

This conclusion can also be expressed through the values of the strength ratio and mass ratio, which are listed in Table 4. These two ratios were used to compare the strongest Sample C and Sample D with the most effective structure. The strength ratio D/C expresses the percentage comparison of the strength of Sample D to the strength of Sample C. It is the same with the mass ratio. Thanks to these ratios, it is possible to express the following conclusion. Specimen D has only 83.04% of the mass of the strongest Specimen C but will carry up to 86.55% of the load compared to Specimen C.

4.3. Analysis of Structural Failures during the Bending Test

Experimental research on the bending stress of specimens of different building structures also showed different types of structure failures. As is known from the theory of three-point bending, the volume below the neutral plane is subjected to tensile stress, while the volume above it is subjected to compressive stress. Experiments have shown that fiber orientation has a great influence not only on flexural strength but also on structural failures.

It should be emphasized that the course of flexural strength during the test was significantly different in Sample A compared to Samples B, C, and D. For Samples B, C, and D, the course was characterized by a continuous increase to a maximum, then a slight decrease after overcoming the strength limit and then a very gradual decrease in the value (Figure 22). This was due to the longitudinal orientation of the fibers in the tensile volume. On the other hand, the course of flexural strength during the test of Sample A was characterized by a continuous increase to the maximum value and a subsequent brittle fracture in the entire cross-section of the specimen (Figure 23). The brittle fracture was caused by the transverse orientation of the fibers along the entire height of the specimen.

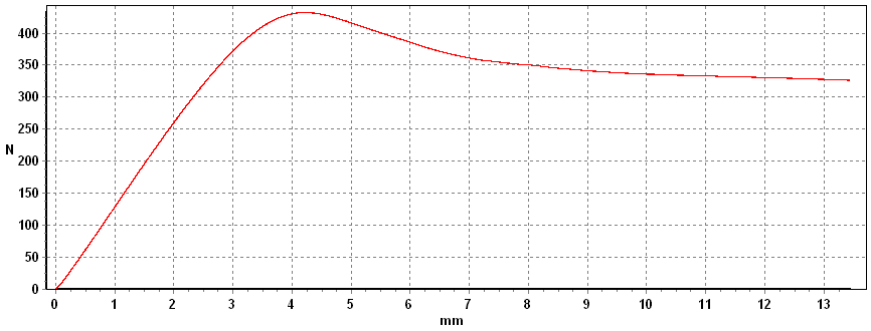

Figure 22. The "force–deformation" curve (trend line) of Samples B, C, and D during the bending test—ends with a plastic extension of the lower layers. All measured curves have very similar characteristics.

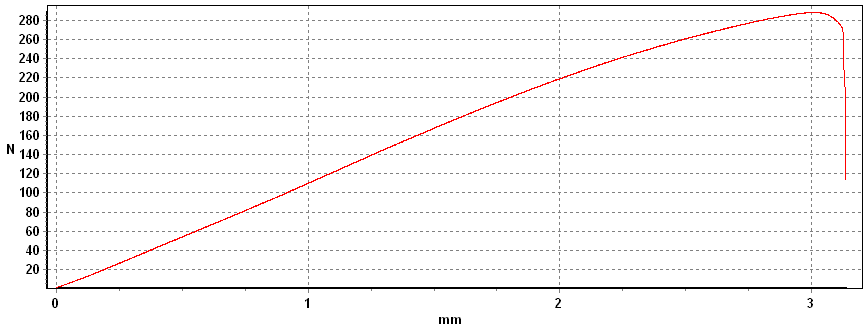

Figure 23. The "force–deformation" curve of Sample A during the bending test—which ended in a brittle fracture.

The structural failures of samples after the bending test are shown in Figure 24. Areas of failure were investigated with a microscope at 33× zoom.

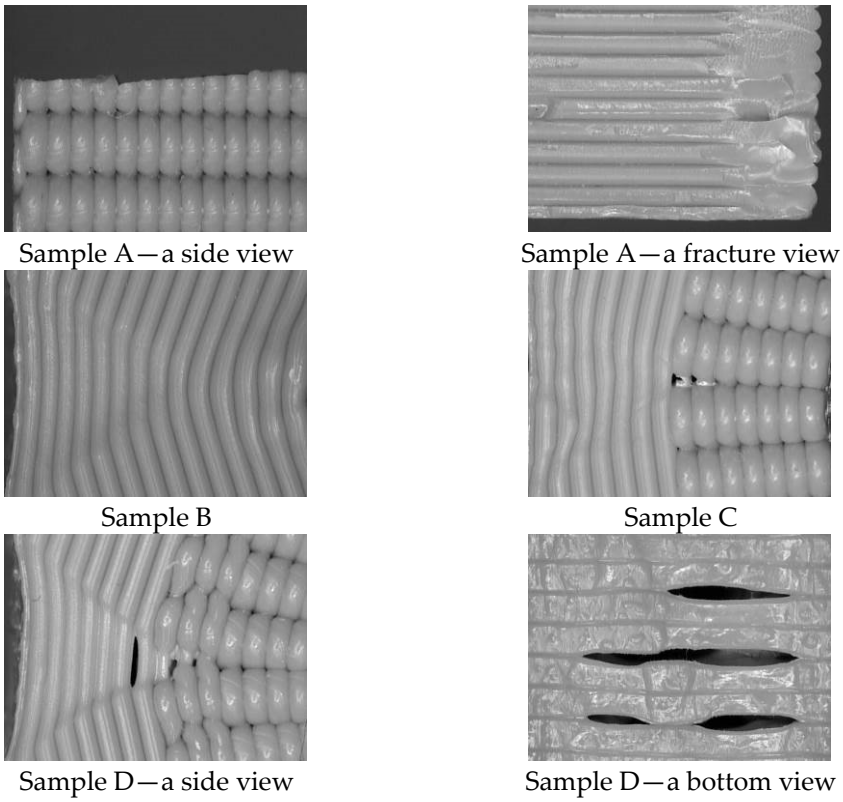

Figure 24. The structural failures investigated at 33× zoom.

Sample A is characterized by a brittle fracture throughout the cross-section. The building structure is formed by fibers placed perpendicular to the neutral axis. As can be seen from Figure 24, the fibers were significantly fused only at the edges. Due to the load, the fibers separated in the vertical plane, and a brittle fracture occurred at the edges.

Samples B and C are characterized by visible fiber pulling below the neutral plane and fiber compression above the neutral plane. Sample B is characterized by a lateral deflection of the compressed volume. Sample C has a shape-stable compressed volume (no lateral deflection); compression fills the volumes between the transverse fibers.

Sample D with a lightened filling has the same failure as Sample C. With greater deformation, the drawn longitudinal fibers separate in the lower layer.

5. Implementation of Experimental Results and FEM Analysis into AM Control

Based on the results of experimental research on the effect of the building structure on flexural strength, it is possible to define and apply an effective combination of the structure of the printed component. The results of the FEM analysis serve to define the volumes in the component with different levels of infill geometry and infill density based on different levels of stress. The FEM simulation also serves to define the effective fiber orientation.

In this case, the methodology of AM control with integrated results was used for developing the G-code for effective production of the real application—drawbar. The developed G-code takes into account the above-mentioned obtained results and enables progressive production while minimizing production time, production costs, and the volume of used material and maintaining the functionality and strength of the component. Figure 25 shows the implementation of FEM simulation into the infill building structure of the drawbar in the section view. The effective fiber orientation based on FEM simulation is shown in Figure 26. The results of the applied methodology are the achievement of symmetrical stress distribution in all partial volumes of the component. This approach allows for maximizing productivity while ensuring the required strength of the component and minimizing costs, production time, and material consumption.

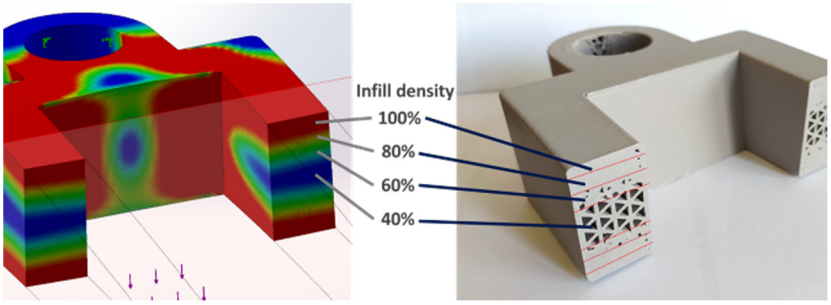

Figure 25. Infill structure and infill density based on the FEM simulation. Warm colors in the FEM simulation output mean a higher stress level, so the actual infill of the component has a higher density. With cold colors, the result is the opposite.

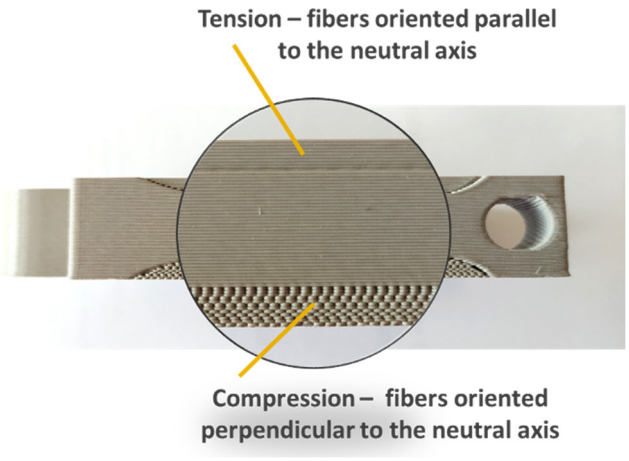

Figure 26. The effective fiber orientation based on FEM simulation.

6. Conclusions

Although additive manufacturing is a progressive technology, the currently applied conservative approach has significant limits. However, these limits can be removed in software by implementing the mentioned methodology of AM control. Integrating the results of this developed methodology into printing software for 3D printers based on FDM technology will significantly help to streamline production. The application of the proposed

methodology significantly reduces production times, costs, the amount of material used, as well as mass while maintaining the required strength and shape. After determining the volumes with different stress levels, these outputs will be integrated into the developing slicer software to design the specific structure of the model and the technological and material parameters of production. For low-stress component volumes, a lightweight infill structure will be designed to save manufacturing time and material. For component volumes with a higher stress level, the software will suggest optimal technological or material parameters. The same approach will be applied to fiber orientations based on the identification of volumes loaded with tensile stress and compressive stress, and the highest effect can be obtained by a combination of both types of results from FEM analysis. With the implementation of optimum infill geometry and density in combination with optimum fiber orientation into the slicer software, it is possible to achieve the production of a highly efficient component in which the stress will be distributed symmetrically. The results of the mentioned experimental research proved that the combined orientation of the fibers, as well as the correctly chosen infill based on the outputs of the FEM simulation, enables highly efficient AM production. This progressive approach makes it possible to generate data for 3D printing based on FEM analysis of components to obtain an optimized printed structure of components and optimized technological and material parameters with regard to maximizing the strength of components and minimizing production times and costs.

Author Contributions: Methodology, M.M. and P.K.; software, S.S.; validation, J.B.; formal analysis, P.K., J.K. and J.B.; investigation, M.M. and J.K.; resources, Ľ.Š.; data curation, S.S. and Ľ.Š.; writing—original draft preparation, M.M.; writing—review and editing, M.M.; visualization, M.M.; supervision, M.M.; project administration, M.M. and P.K.; funding acquisition, M.M. All authors have read and agreed to the published version of the manuscript.

Funding: This research was funded by the Ministry of Education, Science, Research and Sport of the Slovak Republic (grant number VEGA 1/0665/21 and grant number KEGA 033STU-4/2022).

Data Availability Statement: Not applicable.

Acknowledgments: This paper is a part of research conducted within the project VEGA 1/0665/21, „Research and optimization of technological parameters of progressive additive manufacturing of effective protective equipment against COVID-19“ funded by the by the Scientific Grant Agency of the Ministry of Education, Science, Research and Sport of the Slovak Republic and the Slovak Academy of Sciences, within the project KEGA 033STU-4/2022 „Creation and implementation of a certified course for CAx systems with elements of artificial intelligence in the teaching of mechanical engineering“ funded by the Ministry of Education, Science, Research and Sport of the Slovak Republic.

Conflicts of Interest: The authors declare no conflict of interest.

References

1. Bourell, D.; Kruth, J.P.; Leu, M.; Levy, G.; Rosen, D.; Beese, A.M.; Clare, A. Materials for additive manufacturing. *CIRP Ann. Manuf. Technol.* **2017**, *66*, 659–681. [CrossRef]
2. *ISO/ASTM 52900:2021*; Additive Manufacturing—General Principles—Fundamentals and Vocabulary. International Organization for Standardization: Geneva, Switzerland, 2021. Available online: https://www.iso.org/standard/74514.html (accessed on 30 May 2019).
3. *ASTM F2792-10*; Standard Terminology for Additive Manufacturing Technologies. ASTM International: West Conshohocken, PA, USA, 2010.
4. Attaran, M. The rise of 3-D printing: The advantages of additive manufacturing over traditional manufacturing. *Bus. Horiz.* **2017**, *60*, 677–688. [CrossRef]
5. Talagani, M.; DorMohammadi, S.; Dutton, R.; Godines, C.; Baid, H.; Abdi, F.; Kunc, V.; Compton, B.; Simunovic, S.; Duty, C.; et al. Numerical simulation of big area additive manufacturing (3D printing) of a full size car. *SAMPE J.* **2015**, *51*, 27–36.
6. Do, A.V.; Khorsand, B.; Geary, S.M.; Salem, A.K. 3D printing of scaffolds for tissue regeneration applications. *Adv. Healthc. Mater.* **2015**, *4*, 1742–1762. [CrossRef] [PubMed]
7. Zhu, W.; Ma, X.; Gou, M.; Mei, D.; Zhang, K.; Chen, S. 3D printing of functional biomaterials for tissue engineering. *Curr. Opin. Biotechnol.* **2016**, *40*, 103–112. [CrossRef] [PubMed]

8. Wang, M.O.; Vorwald, C.E.; Dreher, M.L.; Mott, E.J.; Cheng, M.H.; Cinar, A.; Mehdizadeh, H.; Somo, S.; Dean, D.; Brey, E.M.; et al. Evaluating 3D-printed biomaterials as scaffolds for vascularized bone tissue engineering. *Adv. Mater.* **2014**, *27*, 138–144. [CrossRef] [PubMed]
9. Blaeser, A.; Campos, D.F.D.; Puster, U.; Richtering, W.; Stevens, M.M.; Fischer, H. Controlling shear stress in 3D bioprinting is a Key factor to balance printing resolution and stem cell integrity. *Adv. Healthc. Mater.* **2016**, *5*, 326–333. [CrossRef]
10. Klocke, F.; Arntz, K.; Teli, M.; Winands, K.; Wegener, M.; Oliari, S. State-of-the-Art Laser Additive Manufacturing for Hotwork Tool Steels. *Procedia CIRP* **2017**, *63*, 58–63. [CrossRef]
11. Gibson, I.; Rosen, D.; Strucker, B.; Khorasani, M. *Additive Manufacturing Technologies*; Springer Nature: Cham, Switzerland, 2021; ISBN 978-3-030-56127-7.
12. Adel, M.; Abdelaal, O.; Gad, A.; Nasr, A.B.; Khalil, A.M. Polishing of fused deposition modeling products by hot air jet: Evaluation of surface roughness. *J. Mater. Process. Technol.* **2018**, *251*, 73–82. [CrossRef]
13. Kartikeyan, B.; Ponshanmugakumar, A.; Saravanan, G.; BharathGanesh, S.; Hemamalini, V. Experimental and theoretical analysis of FDM AM PLA mechanical properties. *Mater. Today Proc.* 2023, *in press*. [CrossRef]
14. B3D-ONLINE 2019, Anon FFF/FDM 3D Print 101-Layer Height, Infill & Support. Available online: https://www.b3d-online.com/blog-news/ffffdm-3d-print-101-layer-height-infill-support (accessed on 30 May 2019).
15. Bergonzi, L.; Vettori, M.; Stefanini, L.; D'Alcamo, L. Different infill geometry influence on mechanical properties of FDM produced PLA. *IOP Conf. Ser. Mater. Sci. Eng.* **2021**, *1038*, 012071. [CrossRef]
16. Beniak, J.; Matúš, M.; Šooš, Ľ.; Križan, P. Strength produced parts by fused deposition modeling. *Glob. J. Eng. Technol. Adv.* **2020**, *5*, 57–62. [CrossRef]
17. Prajapati, A.R.; Dave, H.K.; Raval, H.K. Effect of fiber volume fraction on the impact strength of fiber reinforced polymer composites made by FDM process. *Mater. Today Proc.* **2021**, *44*, 2102–2106. [CrossRef]
18. Dev, S.; Srivastava, R. Optimization of fused deposition modeling (FDM) process parameters for flexural strength. *Mater. Today Proc.* **2021**, *44*, 3012–3016. [CrossRef]
19. Beniak, J.; Križan, P.; Matúš, M. A comparison of the tensile strength of plastic parts produced by a fused deposition modeling device. *Acta Polytech.* **2015**, *55*, 359–365. [CrossRef]
20. Yao, T.; Ye, J.; Deng, Z.; Zhang, K.; Ma, Y.; Ouyang, H. Tensile failure strength and separation angle of FDM 3D printing PLA material: Experimental and theoretical analyses. *Compos. Part B Eng.* **2020**, *188*, 107894. [CrossRef]
21. Ziemian, S.; Okwara, M.; Ziemian, C.W. Tensile and fatigue behavior of layered acrylonitrile butadiene styrene. *Rapid Prototyp. J.* **2015**, *21*, 270–278. [CrossRef]
22. Chacón, J.M.; Caminero, M.A.; García-Plaza, E.; Núñez, P.J. Additive manufacturing of PLA structures using fused deposition modelling: Effect of process parameters on mechanical properties and their optimal selection. *Mater. Des.* **2017**, *124*, 143–157. [CrossRef]
23. Sood, A.K.; Ohdar, R.K.; Mahapatra, S.S. Parametric appraisal of mechanical property of fused deposition modelling processed parts. *Mater. Des.* **2010**, *31*, 287–295. [CrossRef]
24. Ulu, E.; Korkmaz, E.; Yay, K.; Ozdoganlar, O.B.; Kara, L.B. Enhancing the structural performance of additively manufactured objects through build orientation optimization. *J. Mech. Des.* **2015**, *137*, 111410. [CrossRef]
25. Wang, Q.; Zhang, G.; Zheng, X.; Ni, Y.; Liu, F.; Liu, Y.; Xu, L.R. Efficient characterization on the interlayer shear strengths of 3D printing polymers. *J. Mater. Res. Technol.* **2023**, *22*, 2768–2780. [CrossRef]
26. Zou, R.; Xia, Y.; Liu, S.; Hu, P.; Hou, W.; Hu, Q.; Shan, C. Isotropic and anisotropic elasticity and yielding of 3D printed material. *Compos. Part B Eng.* **2016**, *99*, 506–513. [CrossRef]
27. Casavola, C.; Cazzato, A.; Moramarco, V.; Pappalettere, C. Orthotropic mechanical properties of fused deposition modelling parts described by classical laminate theory. *Mater. Des.* **2016**, *90*, 453–458. [CrossRef]
28. Fernandez-Vicente, M.; Calle, W.; Ferrandiz, S.; Conejero, A. Effect of Infill Parameters on Tensile Mechanical Behavior in Desktop 3D Printing 3D. *Print. Addit. Manuf.* **2016**, *3*, 183–192. [CrossRef]
29. Alvarez, C.K.L.; Lagos, C.R.F.; Aizpun, M. Investigating the influence of infill percentage on the mechanical properties of fused deposition modelled ABS parts. *Ing. Investig.* **2016**, *36*, 110–116. [CrossRef]
30. Gopsill, J.A.; Shindler, J.; Hicks, B.J. Using finite element analysis to influence the infill design of fused deposition modelled parts. *Prog. Addit. Manuf.* **2018**, *3*, 145–163. [CrossRef]
31. Khan, S.A.; Siddiqui, B.A.; Fahad, M.; Khan, M.A. Evaluation of the Effect of Infill Pattern on Mechanical Stregnth of Additively Manufactured Specimen. *MSF* **2017**, *887*, 128–132. [CrossRef]
32. Lužanin, O.; Movrin, D.; Plan, M. Effect of layer thickness, deposition angle, and infill on maximum flexural force in FDM-built specimens. *J. Technol. Plast.* **2014**, *39*, 11.
33. Fiuk, G.; Mrzygłód, M. Topology optimization of structures with stress and additive manufacturing constraints. *J. Theor. Appl. Mech.* **2020**, *58*, 459–468. [CrossRef] [PubMed]
34. Feng, Y.; Noda, M.; Noguchi, Y.; Matsushima, K.; Yamada, T. Multi-material topology optimization for additive manufacturing considering dimensional constraints. *Comput. Methods Appl. Mech. Eng.* **2023**, *410*, 116027. [CrossRef]
35. Sung, M.K.; Schwerin, M.; Badhe, Y.; Porter, D. Influence of topology optimization parameters on the mechanical response of an additively manufactured test structure. *J. Mech. Behav. Biomed. Mater.* **2023**, *142*, 105844. [CrossRef]

36. Tajima, M.; Yamada, T. Topology optimization with geometric constraints for additive manufacturing based on coupled fictitious physical model. *Comput. Methods Appl. Mech. Eng.* **2023**, *417*, 116415. [CrossRef]
37. Shimoda, M.; Umemura, M.; Ali, M.; Tsukihara, R. Shape and topology optimization method for fiber placement design of CFRP plate and shell structures. *Compos. Struct.* **2023**, *309*, 116729. [CrossRef]
38. Zhang, J.; An, Q. Topology optimization of fibre reinforced polymer lattice structures for additive manufacturing. *Compos. Sci. Technol.* **2023**, *242*, 110144. [CrossRef]
39. Liu, J.; Huang, J.; Zheng, Y.; Hou, S.; Xu, S.; Ma, Y.; Huang, C.; Zou, B.; Li, L. Challenges in topology optimization for hybrid additive–subtractive manufacturing: A review. *Comput. Aided Des.* **2023**, *161*, 103531. [CrossRef]
40. Matúš, M.; Beniak, J.; Križan, P. Implementation of FEM analysis into additive manufacturing to increase productivity and components strength. *Glob. J. Eng. Technol. Adv.* **2022**, *10*, 87–93. [CrossRef]
41. Vala, J. On a Computational Smeared Damage Approach to the Analysis of Strength of Quasi-Brittle Materials. *WSEAS Trans. Appl. Theor. Mech.* **2021**, *16*, 283–292. [CrossRef]
42. *ISO 178:2019*; Plastics—Determination of Flexural Properties. International Organization for Standardization: Geneva, Switzerland, 2019. Available online: https://www.iso.org/standard/70513.html (accessed on 30 May 2019).